JOC The Journal of Organic Chemistry

pubs.acs.org/joc Article

Electron-Deficient Polycyclic π-System Fused with Multiple B←N Coordinate Bonds

Yirui Cao,[‖] Congzhi Zhu,*[,‖] Maciej Barłóg, Kayla P. Barker, Xiaozhou Ji, Alexander J. Kalin, Mohammed Al-Hashimi,* and Lei Fang*

Cite This: J. Org. Chem. 2021, 86, 2100−2106 Read Online

ACCESS | Metrics & More | Article Recommendations | Supporting Information

ABSTRACT: An extensive polycyclic π-system with 23 fused rings is synthesized via a highly efficient borylation reaction, in which four B−N covalent bonds and four B←N coordinate bonds are formed in one pot. B←N coordinate bonds not only lock the backbone into a near-coplanar conformation but also decrease the LUMO energy level to around −3.82 eV, demonstrating the dual utility of this strategy for the synthesis of extensive rigid polycyclic molecules and the development of *n*-type conjugated materials for organic electronics and organic photovoltaics.

INTRODUCTION

Polycyclic π-systems are ubiquitous in organic molecules that are essential for a wide range of applications including organic electronics, bioimaging, and pharmaceutics.[1−4] In these molecules, the fused-ring constitution of the backbone promotes extensive π-conjugation, enhances the backbone rigidity, and reduces conformation disorder.[5] As a result, polycyclic aromatic molecules typically exhibit narrow optical band gaps, strong intermolecular π-π interactions, and excellent chemical stability.[4]

The synthesis of polycyclic aromatic molecules can be accomplished through either (i) stepwise cross-coupling of smaller molecular building blocks, followed by ring annulation, or (ii) one-step annulative π-extension.[2] The first method, in which an efficient ring-fusing annulation takes place after the assembly of all structural components, is highly versatile and allows for the construction of polycyclic systems with a wide scope of structural diversity. Most known polycyclic aromatic molecules, such as oligoacenes,[6,7] thienoacenes,[8] quinacridones,[9] nanographenes,[10−13] and carbon nanobelts,[14,15] are electron-rich or exhibit *p*-type semiconducting properties. However, it remains challenging to render electron-deficient characteristics to polycyclic aromatic molecules, while electron-deficient polycyclic molecules hold great promise as *n*-type semiconductors in organic electronics and non-fullerene electron acceptors in organic photovoltaics.[16−21] The synthetic challenges include (1) the low reactivity of electron-deficient aromatic units in commonly employed ring-annulation reactions, such as electrophilic aromatic substitution or oxidative C−C coupling, and (2) the limited synthetic methods to precisely functionalize polycyclic aromatic molecules with electron-withdrawing substituents.[22,23] To date, examples of electron-deficient polycyclic arenes are mostly limited to those containing azacene units,[24] or those with pendant electron-withdrawing groups such as imide or cyanide groups.[3,17,20−22,25] Efficient synthetic methodologies and molecular design principles beyond these classes of compounds are desired in order to broaden the structural scope of *n*-type fused-ring π-systems.

Replacing C−C bonds in polycyclic aromatic hydrocarbons with isoelectronic B←N coordinate bonds represents a powerful strategy to modulate their electronic structures, optical properties, and reactivities.[26−36] It typically decreases the energy level of the lowest unoccupied molecular orbital (LUMO), while imposing a smaller impact on the highest occupied molecular orbital (HOMO).[29,37,38] This in turn facilitates intermolecular electron transfer[39] and narrows the optical band gaps of aromatic molecules.[28,29,37] The strength of a B←N coordinate bond can be as high as 30 kcal/mol.[40] Therefore, it can serve as a strong conformational lock to maintain the structural rigidity and desirable molecular conformation, such as a coplanar conformation that is favorable for π-delocalization.[37,40,41] A number of representative B←N bond-containing conjugated compounds demonstrated high electron mobilities and, therefore, emerged as a novel class of *n*-type organic electronic materials.[34,42] Despite recent advances in this field,[26,27,30,35,37,38] it is still challenging to construct extensive polycyclic π-systems fully fused with B←N coordinate bonds, and to achieve deep LUMO levels (below −3.8 eV) in these systems without introducing pendant electron-withdrawing groups.[43−45] Herein, we report a 23-ring-fused polycyclic π-system constructed by simultaneously incorporating four B←N bonds. This extensive π-system

Received: August 25, 2020
Published: January 7, 2021

https://dx.doi.org/10.1021/acs.joc.0c02052
J. Org. Chem. 2021, 86, 2100−2106

features high molecular rigidity, π-delocalization, and electron-deficient characteristic.

RESULTS AND DISCUSSION

In order to construct an extended polycyclic π-system containing multiple B←N coordinate bonds, it is challenging, but crucial, to develop a ring-annulation reaction that can take place at each desirable reaction site with high efficiency. In this context, the target molecule **BN-1** (Figure 1) was designed to

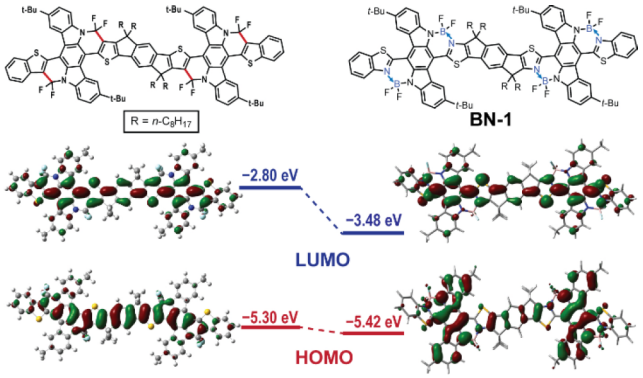

Figure 1. Structural formulas, DFT calculated diagrams, and energy levels of frontier orbitals of **BN-1** featuring multiple B←N coordinate bonds and its structural analogue fused by C−C bonds [B3LYP/6-311G(d,p), isovalue = 0.02].

feature boron dipyrromethene (BODIPY)-like units, in which a boron center is covalently bound to one nitrogen atom (originating from an acidic N−H group) and datively coordinated to another Lewis basic nitrogen atom. To construct these BODIPY-like units in an efficient manner, indolo[3,2-*b*]carbazole was selected as a ditopic N−H donor,[46] instead of aniline analogues that are usually employed in previously reported systems.[44,47] In this case, the stronger acidity of the N−H functionalities in indolo[3,2-*b*]carbazole[48] will better facilitate the formation of covalent B−N bonds in the ring-annulation reaction performed under basic conditions. Moreover, these N−H functionalities are fused with the backbone and thus preorganized to provide the anchoring point for multiple boron centers. Centrosymmetric indaceno[2,1-*d*:6,5-*d*′]dithiazole was selected as the ditopic building block to form the B←N coordinate bonds. The two Lewis basic nitrogen atoms are far away from one another, so that the mutual deactivation on their Lewis basicity is avoided to ensure full installation of all B←N coordinate bonds. The indaceno[2,1-*d*:6,5-*d*′]dithiazole unit also carries four octyl chains to promote the solubility of the final product (Scheme S1).[49] Initial density functional theory (DFT) computation revealed that, in comparison with its structural analogue in which the B←N coordinate bonds are replaced by C−C bonds (Figure 1), the LUMO energy level of **BN-1** was 0.68 eV lower, confirming its electron-deficient characteristics. The orbital diagram showed an extended quinoidal LUMO (Figure 1) and an extended HOMO on the backbone of **BN-1**, facilitated by the nearly coplanar conformation.

The synthesis toward **BN-1** started with a Stille coupling reaction between the dibromo-indolo[3,2-*b*]carbazole derivative **1** and 2-(tri-*n*-butylstannyl)benzo[*d*]thiazole (Figure 2a) to afford a mono-coupled intermediate **2**. The remaining bromide group on **2** was transformed into a pinacol boronic

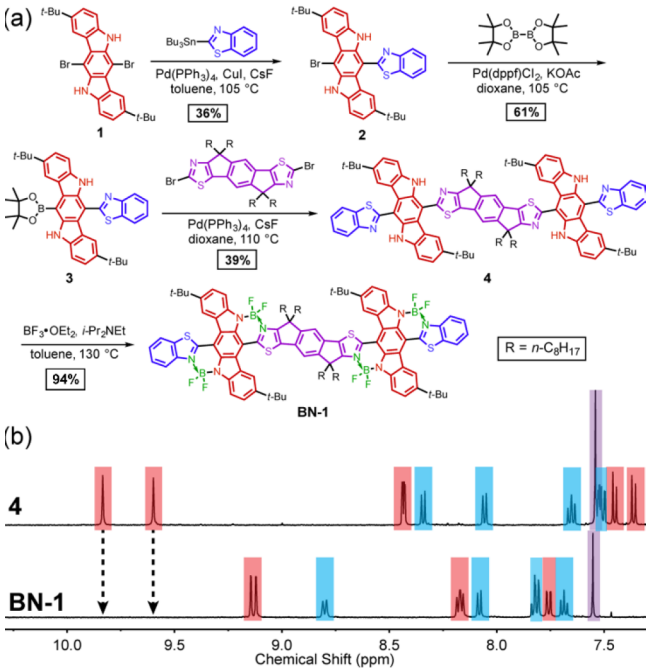

Figure 2. (a) Synthesis of **BN-1**. (b) Comparison of the characteristic ^{1}H NMR (500 MHz) resonance signals of **4** and **BN-1** in $CDCl_3$ at room temperature. The resonance signals from indolo[3,2-*b*]-carbazole units are colored in red, those from benzo[*d*]thiazole units in blue, and the singlet from the central indaceno[2,1-*d*:6,5-*d*′]dithiazole unit in purple.

ester group through Miyaura borylation to give intermediate **3**. Compound **3** was subsequently subjected to Suzuki coupling with the dibrominated indaceno[2,1-*d*:6,5-*d*′]bisthiazole derivative to afford the alternating donor-acceptor-type precursor **4**, which features four acidic N−H functional groups and four Lewis basic thiazole units ready for the borylative annulation to form four BODIPY-like units. Borylation of **4** with BF_3·OEt_2 and *N*,*N*-diisopropylethylamine was performed at 130 °C to give **BN-1** with a remarkable isolated yield of 94%. Compared to previously reported syntheses of polycyclic molecules with multiple B←N coordinate bonds,[34,35,50] the borylation reaction developed here exhibits a much higher conversion owing to the dedicated molecular design principles. The diagnostic disappearance of the N−H resonance signals in the range from 9.5 to 10 ppm suggested a nearly quantitative conversion in this step (Figure 2b). In this reaction, one-pot formation of four B−N covalent bonds and four B←N coordinate bonds took place in each molecule. Despite its rigid structure and extended fused-ring architecture, **BN-1** exhibited an excellent solubility in organic solvents such as chloroform and chlorobenzene.

To better understand the molecular conformation and the nature of the B←N coordinate bonds in **BN-1**, a smaller, yet similar, π-system **BN-2** was synthesized as a model for structural elucidation. The synthesis of **BN-2** was accomplished through an approach similar to that of **BN-1** (Figure 3a). It is noteworthy that the annulation reaction took place at room temperature and afforded **BN-2** in a yield of 94%. Single crystals of **BN-2** suitable for X-ray diffraction structural determination were grown by vapor diffusing pentane into a diluted dichloromethane solution of **BN-2**. In the solid state, **BN-2** showed a rigid and nearly coplanar backbone with a dihedral angle of 9.9° between the indolo[3,2-*b*]carbazole unit

https://dx.doi.org/10.1021/acs.joc.0c02052
J. Org. Chem. 2021, 86, 2100−2106

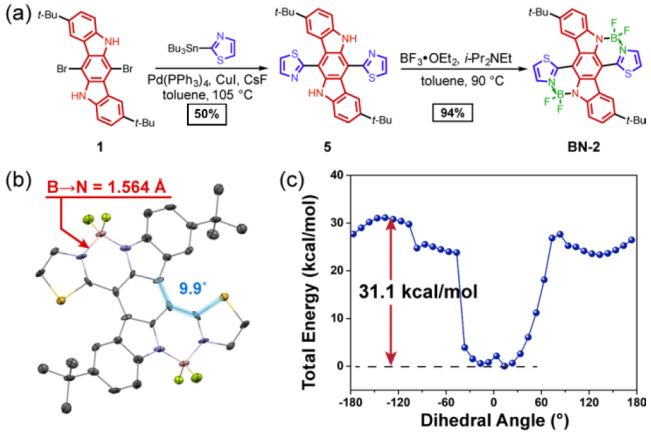

Figure 3. (a) Synthesis of **BN-2**. (b) The single-crystal structure of **BN-2**. (c) The potential energy surface scan of **BN-2** by changing the dihedral angle between indolo[3,2-*b*]carbazole and one of the flanking thiazoles (highlighted in cyan color in (b)).

and the thiazole units (Figure 3b). The conformation twist, although small, was attributed to the steric repulsion between thiazole and indolo[3,2-*b*]carbazole, as evidenced by the short distance (2.460 Å) between the sulfur and the closest hydrogen on the indolo[3,2-*b*]carbazole unit. The bond length of the B←N coordinate bond is 1.564(12) Å, only slightly longer than the B−N covalent bond [1.510(12) Å] (Figure 3b). The formation of such a short B←N coordinate bond was attributed to the resonance effect observed in BODIPY units,[51] which ensures strong B←N coordination and good chemical stability of such compounds. Given the structural similarity between **BN-2** and **BN-1**, it is believed that **BN-1** also adopts a nearly coplanar conformation with a small dihedral angle around 10° between the building blocks.

To evaluate the bond strength of the intramolecular B←N coordinate bonds, the torsional energy landscape of **BN-2** was examined by DFT calculation. The molecular potential energy in the gas phase was computed while the dihedral angle between the central indolo[3,2-*b*]carbazole unit and one of the thiazole units was varied (Figure 3c) from 0° to ±180°. As the dihedral angle deviated from 10°, the potential energy increased, leading to a deep energy well of 30.3 kcal/mol. This value is comparable to the reported complexation enthalpy values between organic bases and BF_3,[52] suggesting a strong coordination between the boron and nitrogen centers, which is sufficient to maintain the extended π-system in a stable rigid conformation.

It was anticipated that the introduction of multiple B←N coordinate bonds can significantly impact the optical properties of conjugated molecules. The photo-absorption onset of precursor **4** is around 590 nm with a λ_{max} of 494 nm. Its fluorescence spectrum exhibits an emission band at 583 nm. In comparison, upon introducing the B←N coordinate bonds, **BN-1** exhibited a red-shifted, intensive absorption band spanning from 600 to 800 nm (λ_{max} = 700 nm) in $CHCl_3$ solution, corresponding to the narrowed band gap of the HOMO to LUMO transition (Figures 4a and S11). The fluorescence emission band of **BN-1** in $CHCl_3$ was found to be centered at 723 nm, which was also red-shifted compared to that of **4**. It is also worthy to note that the Stokes shift of **BN-1** was much smaller than that of **4**, indicating the less significant vibrational energy loss in its excited state due to the rigid structure of **BN-1** (Figure 4a). Compared to **BN-1**, the

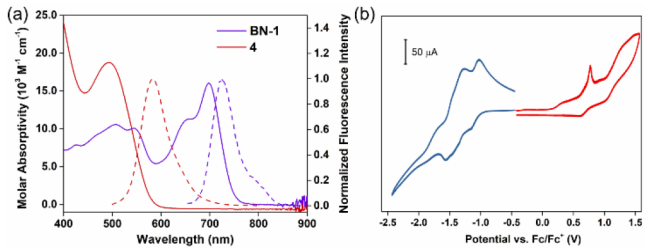

Figure 4. (a) UV−vis−NIR absorption spectra (solid lines) fluorescence emission spectra (dashed lines) of **BN-1** and **4** in a diluted $CHCl_3$ solution. (b) Cyclic voltammogram of a **BN-1** thin film.

absorption spectrum and fluorescence emission spectrum of **BN-2** were blue-shifted, on account of its smaller size of π-conjugation (Figure S17). The quantum yields of **BN-1** and **BN-2** in chloroform were estimated to be 6.6% and 12.9%, respectively, using zinc phthalocyanine as a standard. The absorption spectrum of **BN-1** was also measured in the thin film state, thanks to its good solubility and film-forming ability (Figure S20). The solid-state spectrum was similar to that in solution, suggesting that no significant intermolecular aggregation or conformational changes took place from the solution phase to the solid state for **BN-1**, further corroborating its rigid backbone. Grazing incidence wide-angle X-ray diffraction of the thin film showed ring-like diffraction patterns, revealing the semi-crystalline character of **BN-1** (Figure S12), suggesting the weak π-π interactions between these molecules in the thin film.

The solvatochromism of **BN-1** and **BN-2** was examined in a series of organic solvents. Unlike many reported BODIPY dyes whose absorption maxima were insensitive to solvent polarity changes or show slight shifts of only 2−10 nm,[53,54] significant solvatochromsim was observed for **BN-1** and **BN-2** (Figures S18 and S19). For both compounds, it was observed that, as the solvent polarity increased, the absorption and emission spectra underwent blue shifts. For instance, the λ_{max} of the absorption of **BN-2** was shifted from 645 to 611 nm when the solvent was changed from toluene to dimethylformamide. Such a significant solvatochromism revealed the strong solvation effect on the ground state of **BN-1** and **BN-2** in polar solvents, as a result of the intramolecular charge transfer character in these rigid conjugated molecules.

The introduction of intramolecular B←N coordinate bonds was expected to increase the electron affinity of conjugated molecules. Cyclic voltammetry was performed on a thin film of **BN-1**, which was drop-casted on the surface of a glassy carbon electrode. **BN-1** underwent two semi-reversible reduction processes in the range from −1.6 to −1.0 V vs the ferrocene/ferrocenium redox couple (Figure 4b). Multiple redox processes were also observed on differential pulse voltammetry (Figure S15). The reduction peak of **BN-1** shifted cathodically for 0.46 V compared to that of compound **4** (Figure S13). The LUMO energy level of **BN-1** was determined to be −3.82 eV, much lower than that of **4** (−3.36 eV in Table S6), and close to those of high-performance *n*-type organic semiconductors[18,19,47] and non-fullerene acceptors in organic photovoltaics.[16,17]

CONCLUSION

In conclusion, we established the molecular design and synthesis of an extensive electron-deficient polycyclic π-system

https://dx.doi.org/10.1021/acs.joc.0c02052
J. Org. Chem. 2021, 86, 2100−2106

featuring multiple B←N coordinate bonds. A 23-ring-fused molecule was constructed via a highly efficient borylation reaction, in which four B−N covalent bonds and four B←N coordinate bonds were formed in one pot. The high efficiency in simultaneously fusing multiple rings promises its utility in future synthesis of B←N bridged ladder polymers. These B←N coordinate bonds not only rigidified the backbone and promoted a near-coplanar conformation but also decreased the LUMO energy level to −3.82 eV and led to the intensive absorption in the near-infrared region. This work unveiled that the introduction of multiple B←N coordinate bonds serves dual purposes of (i) fusing the π-system into a rigid polycyclic constitution and (ii) imparting *n*-type characters for the development of new organic molecules and macromolecules for electronic and photovoltaic applications.

EXPERIMENTAL SECTION

Materials and Methods. Starting materials and reagents were purchased from commercial sources and were used as received without further purification. THF was dried and distilled under nitrogen from sodium using benzophenone as the indicator. Toluene was dried using an inert pure solvent system and used without further treatment. An oil bath was used for those reactions that required heating. 6,12-Dibromo-2,8-di-*tert*-butyl-5,11-dihydroindolo[3,2-*b*]-carbazole (**1**) and 2,7-bis(triisopropylsilyl)-*s*-indaceno[2,1-*d*:6,5-*d*′]-bis(thiazole)-4,9-dione were prepared according to reported procedures.[27,55] ^{1}H and ^{13}C{^{1}H} NMR spectra were recorded on a 500 MHz or 400 MHz spectrometer. The ^{1}H and ^{13}C{^{1}H} NMR chemical shifts were reported in ppm relative to the signals corresponding to the residual non-deuterated solvents ($CDCl_3$: ^{1}H 7.26 ppm, ^{13}C 77.23 ppm) or the internal standard (tetramethylsilane: ^{1}H 0.00 ppm). The ^{19}F NMR chemical shifts were reported in ppm relative to the signal corresponding to $BF_3{\cdot}OEt_2$ (−153.0 ppm) as the external standard. Abbreviations for reported signal multiplicities are as follows: s, singlet; d, doublet; t, triplet; q, quartet; m, multiplet; br, broad. The broad singlet at ∼1.55 ppm on ^{1}H NMR spectra represents the resonance signal of H_2O in $CDCl_3$. High-resolution mass spectra were obtained via electrospray ionization (ESI), atmospheric pressure chemical ionization (APCI) with a hybrid quadrupole-orbitrap analyzer, or matrix-assisted laser desorption ionization (MALDI) mode with a time-of-flight analyzer. Column chromatography was carried out on a normal phase SiO_2. Preparative size exclusive chromatography (SEC) purifications were performed at room temperature using chloroform as the eluent at a flow rate of 14 mL/min. UV−vis absorption spectra were recorded in a 1.0 cm path-length cuvette, and the neat solvent was used as baseline. Fluorescence emission spectra were recorded in a 1.0 cm path-length cuvette. Cyclic voltammetry was carried out in nitrogen-purged acetonitrile at room temperature. Tetra-*n*-butylammonium hexafluorophosphate (0.1 M) was used as the supporting electrolyte. The conventional three-electrode configuration consists of an ITO working electrode, a platinum wire anxiliary electrode, and a Ag/AgCl electrode with ferrocenium/ferrocene as the standard. Cyclic voltammograms were obtained at a scan rate of 200 mV/s. The absorption spectra of **4** and **BN-1** were recorded at room temperature at concentrations of 2.2×10^{-5} M and 2.1×10^{-5} M, respectively. The emission spectra of **4** and **BN-1** were recorded at room temperature at concentrations of 2.2×10^{-6} M and 2.1×10^{-5} M, respectively. The excitation wavelengths for **4** and **BN-1** were set at 620 and 650 nm, respectively.

2-(12-Bromo-2,8-di-*tert*-butyl-5,11-dihydroindolo[3,2-*b*]-carbazol-6-yl)benzo[*d*]thiazole (2). **1** (690 mg, 1.31 mmol) and tri-*n*-butylstannylbenzothiazole (680 mg, 2.28 mmol) were suspended in toluene (13 mL). The suspension was degassed by three cycles of freeze-pump-thaw before $Pd(PPh_3)_4$ (151 mg, 0.13 mmol), CuI (12.5 mg, 0.066 mmol), and CsF (996 mg, 6.55 mmol) were added under N_2. The reaction mixture was stirred at 105 °C for 36 h. After cooling to room temperature, the mixture was extracted with CH_2Cl_2 and washed with 1 M HCl once, brine twice, water once, and dried with $MgSO_4$. Volatile solvents were removed under reduced pressure. The crude product was purified through column chromatography (SiO_2, hexane/CH_2Cl_2 1:1 to 1:9) to give **2** as an orange solid (96.2 mg, 36%). ^{1}H NMR (400 MHz, $CDCl_3$) δ = 9.69 (s, 1H), 8.84 (d, J = 1.6 Hz, 1H), 8.38 (d, J = 1.6 Hz, 1H), 8.36 (s, 1H), 8.29 (d, J = 7.6 Hz, 1H), 8.03 (d, J = 7.6 Hz, 1H), 7.63 (m, 1H), 7.53 (m, 3H), 7.45 (d, J = 8.0 Hz, 1H), 7.36 (d, J = 8.0 Hz, 1H), 1.51 (s, 9H), 1.32 (s, 9H). ^{13}C{^{1}H} NMR (100 MHz, $CDCl_3$) δ = 164.5, 153.6, 142.5, 142.2, 139.2, 139.0, 136.1, 135.6, 134.9, 126.7, 125.8, 125.2, 125.1, 123.5, 122.6, 122.6, 121.8, 121.8, 120.6, 120.3, 118.7, 110.6, 110.4, 108.6, 100.7, 35.0, 32.2, 32.1. APCI-MS: m/z [M + H]$^+$ Calcd for $C_{33}H_{31}N_3SBr$ 580.1417; Found 580.1400.

2-(2,8-Di-*tert*-butyl-12-(4,4,5,5-tetramethyl-1,3,2-dioxaborolan-2-yl)-5,11-dihydroindolo[3,2-*b*]carbazol-6-yl)benzo[*d*]-thiazole (3). **2** (106 mg, 0.18 mmol), bis(pinacolato)diboron (91 mg, 0.36 mmol), and KOAc (35 mg, 0.36 mmol) were suspended in dioxane (3 mL). The suspension was degassed by three cycles of freeze-pump-thaw before $Pd(dppf)Cl_2$ (13 mg, 0.018 mmol) was added under N_2. The reaction mixture was stirred at 105 °C for 36 h. After cooling to room temperature, the mixture was extracted with CH_2Cl_2 and washed with 1 M HCl once, brine twice, water once, and dried with $MgSO_4$. Volatile solvents were removed under reduced pressure. The product was purified through preparative size exclusion chromatography to give compound **3** as an orange solid (69 mg, 61%). ^{1}H NMR (400 MHz, $CDCl_3$) δ = 9.95 (s, 1H), 9.50 (s, 1H), 9.04 (d, J = 2.0 Hz, 1H), 8.33 (d, J = 8.4 Hz, 1H), 8.28 (d, J = 2.0 Hz, 1H), 8.04 (d, J = 7.6 Hz, 1H), 7.64 (m, 1H), 7.53−7.50 (m, 3H), 7.48 (d, J = 8.4 Hz, 1H), 7.37 (d, J = 8.4 Hz, 1H), 1.61 (s, 12H), 1.50 (s, 9H), 1.29 (s, 9H). ^{13}C{^{1}H} NMR (100 MHz, $CDCl_3$) δ = 165.2, 153.7, 143.9, 141.8, 141.0, 139.6, 135.9, 134.9, 128.6, 126.6, 125.8, 124.5, 123.9, 123.6, 121.8, 121.8, 121.0, 119.8, 119.3, 112.5, 110.1, 109.9, 84.4, 35.2, 34.9, 32.5, 32.1, 25.6. APCI-MS: m/z [M + H]$^+$ Calcd for $C_{39}H_{43}BN_3O_2S$ 628.3164; Found 628.3150.

Compound 4. **3** (75.0 mg, 0.12 mmol) and 2,7-dibromo-4,4,9,9-tetraoctyl-4,9-dihydro-*s*-indaceno[2,1-*d*:6,5-*d*′]bis(thiazole) (26.0 mg, 0.03 mmol) were suspended in anhydrous dioxane (2.0 mL) at room temperature. The suspension was degassed by three cycles of freeze-pump-thaw before $Pd(PPh_3)_4$ (3.5 mg, 0.003 mmol) and CsF (45.6 mg, 0.3 mmol) were added under N_2. The reaction mixture was stirred at 110 °C for 48 h. After cooling to room temperature, the mixture was extracted with CH_2Cl_2 and washed with 1 M HCl once, brine twice, water once, and dried with $MgSO_4$. Volatile solvents were removed under reduced pressure. After purification through column chromatography (SiO_2, hexane/CH_2Cl_2 1:1 to 1:9), all the red-colored solution that showed orange-colored fluorescence under a 365 nm UV lamp was collected. Volatile solvents were removed under reduced pressure to yield the crude product. The product was further purified through preparative size exclusion chromatography to give compound **4** as a red solid (20.0 mg, 39%). ^{1}H NMR (500 MHz, $CDCl_3$) δ = 9.86 (s, 2H), 9.62 (s, 2H), 8.46 (d, J = 2.0 Hz, 2H), 8.45 (d, J = 2.0 Hz, 2H), 8.37 (m, 2H), 8.08 (m, 2H), 7.67 (td, J = 8.0, 1.5 Hz, 2H), 7.57−7.52 (m, 6H), 7.56 (s, 2H), 7.47 (d, J = 8.5 Hz, 2H), 7.38 (d, J = 8.5 Hz, 2H), 2.45 (m, 4H), 2.18 (m, 4H), 1.36 (s, 18H), 1.33 (s, 18H), 1.25−1.15 (m, 48H), 0.80 (t, J = 7.0 Hz, 12H). ^{13}C{^{1}H} NMR (100 MHz, $CDCl_3$) δ = 170.7, 164.9, 153.6, 152.7, 141.8, 141.7, 139.5, 139.5, 136.3, 136.0, 135.9, 135.7, 134.7, 126.7, 125.8, 125.0, 124.9, 123.6, 121.9, 120.9, 120.6, 120.2, 119.7, 115.3, 113.0, 111.0, 110.8, 110.6, 53.6, 38.5, 35.0, 32.1, 32.0, 31.8, 30.4, 29.8, 29.6, 28.1, 27.3, 24.8, 22.8, 14.3. ESI-MS: m/z [M + H]$^+$ Calcd for $C_{112}H_{131}N_8S_4$ 1719.9413; Found 1719.9439.

BN-1. In a N_2-filled glovebox, **4** (20.0 mg, 0.012 mmol), anhydrous toluene (1.0 mL), diisopropylethylamine (0.1 mL), and $BF_3{\cdot}OEt_2$ (0.2 mL, 1.6 mmol) were added into a thick-walled reaction vessel, which was subsequently screw-sealed with a PTFE cap. The reaction mixture was stirred at 115 °C for 48 h and at 130 °C for 48 h. After completion of the reaction, the reaction was cooled to room temperature, and volatile solvents were removed under reduced pressure. The crude product was dissolved in CH_2Cl_2 (30 mL). To this solution, methanol (20 mL) was added. The mixture was stirred

https://dx.doi.org/10.1021/acs.joc.0c02052
J. Org. Chem. 2021, 86, 2100−2106

at room temperature for 30 min. CH_2Cl_2 was removed under reduced pressure using a rotary evaporator, affording a suspension of **BN-1** in methanol. The suspension was collected by filtration and washed with excessive methanol at room temperature to give **BN-1** as a deep-purple solid (19.0 mg, 94%). ^{1}H NMR (500 MHz, $CDCl_3$) δ = 9.14 (d, J = 2.0 Hz, 2H), 9.12 (d, J = 2.0 Hz, 2H), 8.80 (d, J = 8.5 Hz, 2H), 8.17 (m, 4H), 8.08 (d, 2H), 7.84−7.80 (m, 4H), 7.77−7.75 (dd, J = 8.5, 2.0 Hz, 6H), 7.47 (td, J = 8.0, 1.0 Hz, 2H), 7.55 (s, 2H), 3.07 (m, 4H), 2.23 (m, 4H), 1.64 (s, 18H), 1.25 (s, 18H), 1.25−1.07 (m, 48H), 0.7 (t, J = 7.0 Hz, 12H). ^{13}C{^{1}H} NMR (125 MHz, $CDCl_3$) δ = 165.1, 164.5, 162.7, 154.3, 143.9, 143.0, 143.0, 142.7, 142.6, 138.7, 137.6, 136.0, 133.8, 129.9, 129.3, 127.7, 126.7, 122.1, 121.7, 121.6, 120.0, 119.5, 119.3, 118.8, 114.6, 114.0, 111.3, 108.1, 58.7, 38.1, 35.7, 35.5, 32.3, 32.3, 31.9, 29.8, 29.4, 29.3, 24.3, 22.7, 14.2. ^{19}F NMR (470.4 MHz, $CDCl_3$) δ = 133.23 (m), 135.39 (m). MALDI-MS: m/z $[M]^+$ Calcd for $C_{112}H_{126}N_8S_4B_4F_8$ 1907.9266; Found 1907.9115.

2,2′-(2,8-Di-*tert*-butyl-5,11-dihydroindolo[3,2-*b*]carbazole-6,12-diyl)dithiazole (5). 6,12-Dibromo-2,8-di-*tert*-butyl-5,11-dihydroindolo[3,2-*b*]carbazole (**1**) (52.5 mg, 0.10 mmol) and 2-(tributylstannyl)thiazole (158.3 mg, 0.30 mmol) were added into toluene (1.0 mL). The suspension was degassed by three cycles of freeze-pump-thaw before $Pd(PPh_3)_4$ (11.6 mg, 0.010 mmol), CuI (3.8 mg, 0.020 mmol), and CsF (91.1 mg, 0.60 mmol) were added under N_2. The reaction mixture was stirred at 110 °C for 48 h. After cooling to room temperature, the mixture was extracted with CH_2Cl_2 and washed with 1 M HCl once, brine twice, water once, and dried with $MgSO_4$. The crude product was purified through column chromatography (SiO_2, hexane/ethyl acetate 9:1 to 7:3) to give **5** as a yellow solid (29.0 mg, 50%). ^{1}H NMR (500 MHz, $CDCl_3$) δ = 9.69 (s, 2H), 8.23 (d, J = 2.0 Hz, 2H), 8.22 (d, J = 3.5 Hz, 2H), 7.68 (d, J = 3.5 Hz, 2H), 7.50 (dd, J = 8.5 Hz, 2.0 Hz, 2H), 7.39 (d, J = 8.5 Hz, 2H), 1.35 (s, 18H). ^{13}C{^{1}H} NMR (125 MHz, $CDCl_3$) δ = 164.5, 143.4, 141.6, 139.5, 135.7, 124.8, 121.8, 120.8, 120.2, 119.5, 111.2, 110.6, 35.0, 32.1. ESI-MS: m/z $[M + H]^+$ Calcd for $C_{32}H_{31}N_4S_2$ 535.1985; Found 535.1983.

2,2′-(2,8-Di-*tert*-butyl-5,11-bis(difluoroboraneyl)-5,11-dihydroindolo[3,2-*b*]carbazole-6,12-diyl)dithiazole (BN-2). In a N_2-filled glovebox, **3** (53.5 mg, 0.10 mmol), anhydrous CH_2Cl_2(5 mL), triethylamine (0.2 mL), and BF_3·OEt_2 (0.3 mL, 2.4 mmol) were added into a thick-walled reaction vessel, which was subsequently screw-sealed by a PTFE cap. The mixture was stirred at room temperature for 24 h. After completion of the reaction, the mixture was extracted with CH_2Cl_2 and washed with 1 M HCl once, brine twice, water once, and dried with $MgSO_4$. The crude product was purified through column chromatography (SiO_2, hexane/ethyl acetate 9:1 to 1:2) to give **BN-2** as a blue solid (59.3 mg, 94%). ^{1}H NMR (500 MHz, $CDCl_3$) δ = 8.93 (d, J = 2.0 Hz, 2H), 8.37 (d, J = 3.5 Hz, 2H), 8.03 (d, J = 8.5 Hz, 2H), 7.75 (d, J = 3.5 Hz, 2H), 7.71 (dd, J = 8.5 Hz, 2.0 Hz, 2H), 1.25 (s, 18H). ^{13}C{^{1}H} NMR was not obtained for **BN-2**, due to its limited solubility. ^{19}F NMR (470.4 MHz, $CDCl_3$) δ = 137.81 (m). APCI-MS: m/z $[M + H]^+$ Calcd for $C_{32}H_{29}N_4S_2B_2F_4$ 631.1945; Found 631.1950. Melting point: 304−310 °C

4,9-Dioctylidene-2,7-bis(triisopropylsilyl)-4,9-dihydro-*s*-indaceno[2,1-*d*:6,5-*d*′]bis(thiazole) (S1). Octyltriphenylphosphonium bromide (728 mg, 1.6 mmol) was dissolved in anhydrous THF (20 mL) at −78 °C. *n*-BuLi (1.0 mL, 1.6 M in hexane) was added dropwise. The mixture was stirred at −78 °C for 1 h. To the cooled mixture at −78 °C, a solution of 2,7-bis(triisopropylsilyl)-*s*-indaceno-[2,1-*d*:6,5-*d*′]bis(thiazole)-4,9-dione (366 mg, 0.60 mmol) in anhydrous THF (15 mL) was added dropwise over 30 min. After the addition, the mixture was stirred at −78 °C for 1 h and slowly warmed up to room temperature. The reaction mixture was further stirred at room temperature overnight. The reaction mixture was extracted with CH_2Cl_2 and washed with brine three times. The organic solution was dried over $MgSO_4$ and concentrated under reduced pressure. The residue was further purified through column chromatography (SiO_2, hexane/CH_2Cl_2 9:1) to give the product as a yellow solid. The product was identified as a mixture of three stereoisomers. One of the isomers was purified by column chromatography and characterized as follows. ^{1}H NMR (400 MHz, $CDCl_3$) δ = 7.67 (s, 2H), 6.77 (t, J = 8.0 Hz, 2H), 3.20 (q, J = 7.6 Hz, 4H), 1.63 (qunitet, J = 7.6 Hz, 4H), 1.48 (septet, J = 7.6 Hz, 6H), 1.40−1.25 (m, 20H), 1.20 (septet, J = 7.6 Hz, 36H), 0.87 (t, J = 6.8 Hz, 6H). ^{13}C{^{1}H} NMR (100 MHz, $CDCl_3$) δ = 171.3, 162.9, 140.5, 140.3, 132.5, 131.2, 130.8, 112.8, 32.1, 29.8, 29.4, 22.9, 18.8, 14.3, 12.0. ESI-MS: m/z $[M + H]^+$ Calcd for $C_{48}H_{77}N_2S_2Si_2$ 801.5061; Found 801.5058. All the isomers were combined (293 mg, 61%) and were used directly in the next step of the synthesis.

4,4,9,9-Tetraoctyl-2,7-bis(triisopropylsilyl)-4,9-dihydro-*s*-indaceno[2,1-*d*:6,5-*d*′]bis(thiazole) (S2). To a suspension of $LiAlH_4$ in anhydrous THF (6 mL) at 0 °C, 1-bromooctane (868 mg, 4.5 mmol) was added. A solution of **S1** (366 mg, 0.45 mmol) in anhydrous THF (6.0 mL) was added dropwise. The mixture was stirred at 0 °C for 1 h and subsequently at 50 °C for 8 h. The solvent was then removed under reduced pressure. The residue was dissolved in CH_2Cl_2 and washed with water twice and dried with $MgSO_4$. After removing the solvent under reduced pressure, the crude product was purified through column chromatography (SiO_2, hexane/CH_2Cl_2 9:1 to 7:1) to afford **S2** as a pale yellow solid (297 mg, 64%). ^{1}H NMR (400 MHz, $CDCl_3$) δ = 7.36 (s, 2H), 2.22 (m, 4H), 1.89 (m, 4H), 1.49 (septet, J = 7.6 Hz, 6H), 1.3−1.0 (m, 76H), 0.9−0.7 (m, 20H). ^{13}C{^{1}H} NMR (125 MHz, $CDCl_3$) δ = 174.0, 171.3, 153.2, 137.3, 134.3, 115.4, 52.8, 38.4, 32.1, 30.1, 29.5, 29.3, 24.2, 22.8, 18.8, 18.8, 14.3, 12.0. ESI-MS: m/z $[M + H]^+$ Calcd for $C_{64}H_{113}N_2S_2Si_2$ 1029.7878; Found 1029.7887.

2,7-Dibromo-4,4,9,9-tetraoctyl-4,9-dihydro-*s*-indaceno[2,1-*d*:6,5-*d*′]bis(thiazole) (S3). **S2** (206 mg, 0.20 mmol) was dissolved in a mixture of THF (4.0 mL) and MeOH (2.0 mL) at room temperature. A solution of TBAF (2.0 mL, 1.0 M in THF) was added dropwise. The mixture was stirred at 55 °C for 16 h. After cooling to room temperature, the mixture was extracted with CH_2Cl_2 and washed with brine twice, water once, and dried with $MgSO_4$. After removing the solvent under reduced pressure, the deprotected product was used without further purification in the next step. It was dissolved in $CHCl_3$ (6 mL) at 0 °C. NBS (85 mg, 0.50 mmol) was added portion-wise. The reaction mixture was then stirred at room temperature for 24 h. After completion of the reaction, the mixture was extracted with CH_2Cl_2 and washed with 1 M HCl once, brine twice, water once, and dried with $MgSO_4$. The crude product was purified through column chromatography (SiO_2, hexane/CH_2Cl_2 9:1 to 4:1) to give **S3** as a pale yellow solid (113 mg, 65%). ^{1}H NMR (400 MHz, $CDCl_3$) δ = 7.28 (s, 2H), 2.15 (m, 4H), 1.88 (m, 4H), 1.20−1.07 (m, 40 H), 0.82−0.73 (m, 20H). ^{13}C{^{1}H} NMR (100 MHz, $CDCl_3$) δ = 168.4, 151.5, 137.2, 135.4, 134.0, 115.0, 54.3, 38.2, 32.0, 30.0, 29.5, 29.4, 24.1, 22.8, 14.3. APCI-MS: m/z $[M + H]^+$ Calcd for $C_{46}H_{71}N_2S_2Br_2$ 875.3405; Found 875.3363. Melting point: 146−147 °C

■ ASSOCIATED CONTENT

Supporting Information

The Supporting Information is available free of charge at https://pubs.acs.org/doi/10.1021/acs.joc.0c02052.

General methods, synthesis details, spectroscopic characterization, cyclic voltammetry data, computation results, and single-crystal analysis conditions (PDF)

Crystallographic data (CIF)

Accession Codes

CCDC 2015357 contains the supplementary crystallographic data for this paper. These data can be obtained free of charge via www.ccdc.cam.ac.uk/data_request/cif, or by emailing data_request@ccdc.cam.ac.uk, or by contacting The Cambridge Crystallographic Data Centre, 12 Union Road, Cambridge CB2 1EZ, UK; fax: +44 1223 336033.

https://dx.doi.org/10.1021/acs.joc.0c02052
J. Org. Chem. 2021, 86, 2100−2106

AUTHOR INFORMATION

Corresponding Authors

Congzhi Zhu − *Department of Chemistry, Texas A&M University, College Station, Texas 77843, United States;* orcid.org/0000-0002-1302-7187; Email: congzhi.zhu@austin.utexas.edu

Mohammed Al-Hashimi − *Department of Chemistry, Texas A&M University at Qatar, Doha, Qatar;* orcid.org/0000-0001-6015-2178; Email: hashimi@tamu.edu

Lei Fang − *Department of Chemistry and Department of Materials Science and Engineering, Texas A&M University, College Station, Texas 77843, United States;* orcid.org/0000-0003-4757-5664; Email: fang@chem.tamu.edu

Authors

Yirui Cao − *Department of Chemistry, Texas A&M University, College Station, Texas 77843, United States*

Maciej Barłóg − *Department of Chemistry, Texas A&M University at Qatar, Doha, Qatar*

Kayla P. Barker − *Department of Chemistry, Texas A&M University, College Station, Texas 77843, United States*

Xiaozhou Ji − *Department of Chemistry, Texas A&M University, College Station, Texas 77843, United States*

Alexander J. Kalin − *Department of Chemistry, Texas A&M University, College Station, Texas 77843, United States*

Complete contact information is available at: https://pubs.acs.org/10.1021/acs.joc.0c02052

Author Contributions

[‖]C.Z. and Y.C. contributed equally.

Notes

The authors declare no competing financial interest.

ACKNOWLEDGMENTS

We acknowledge the National Science Foundation (Award #1654029) and Qatar National Priority Research Program (NPRP11S-1204-170062) for financial support of this work. We also thank Dr. Nattamai Bhuvanesh for X-ray diffraction measurements, and the Laboratory for Molecular Simulation at TAMU for providing software, support, and computer time. We thank Dr. Yi Liu at the Molecular Foundry for providing valuable intellectual inputs to this research. Work at the Molecular Foundry was supported by the Office of Science, Office of Basic Energy Sciences, of the U.S. Department of Energy under Contract No. DE-AC02-05CH11231. We thank Dr. Joe Strzalka for supporting this research at the Advanced Photon Source, a U.S. Department of Energy (DOE) Office of Science User Facility operated for the DOE Office of Science by Argonne National Laboratory under Contract No. DE-AC02-06CH11357.

REFERENCES

(1) Ito, H.; Ozaki, K.; Itami, K. Annulative π-Extension (APEX): Rapid Access to Fused Arenes, Heteroarenes, and Nanographenes. *Angew. Chem., Int. Ed.* **2017**, *56*, 11144−11164.

(2) Ito, H.; Segawa, Y.; Murakami, K.; Itami, K. Polycyclic Arene Synthesis by Annulative π-Extension. *J. Am. Chem. Soc.* **2019**, *141*, 3−10.

(3) Miao, Q. *Polycyclic Arenes and Heteroarenes: Synthesis, Properties, and Applications*; John Wiley & Sons, 2015.

(4) Zhang, L.; Cao, Y.; Colella, N. S.; Liang, Y.; Brédas, J.-L.; Houk, K. N.; Briseno, A. L. Unconventional, Chemically Stable, and Soluble Two-Dimensional Angular Polycyclic Aromatic Hydrocarbons: From Molecular Design to Device Applications. *Acc. Chem. Res.* **2015**, *48*, 500−509.

(5) Zhu, C.; Kalin, A. J.; Fang, L. Covalent and Noncovalent Approaches to Rigid Coplanar π-Conjugated Molecules and Macromolecules. *Acc. Chem. Res.* **2019**, *52*, 1089−1100.

(6) Cai, Z.; Awais, M. A.; Zhang, N.; Yu, L. Exploration of Syntheses and Functions of Higher Ladder-Type π-Conjugated Heteroacenes. *Chem.* **2018**, *4*, 2538−2570.

(7) Bendikov, M.; Wudl, F.; Perepichka, D. F. Tetrathiafulvalenes, Oligoacenenes, and Their Buckminsterfullerene Derivatives: The Brick and Mortar of Organic Electronics. *Chem. Rev.* **2004**, *104*, 4891−4946.

(8) Zheng, T.; Cai, Z.; Ho-Wu, R.; Yau, S. H.; Shaparov, V.; Goodson, T.; Yu, L. Synthesis of Ladder-Type Thienoacenes and Their Electronic and Optical Properties. *J. Am. Chem. Soc.* **2016**, *138*, 868−875.

(9) Daniel Głowacki, E.; Leonat, L.; Irimia-Vladu, M.; Schwödiauer, R.; Ullah, M.; Sitter, H.; Bauer, S.; Serdar Sariciftci, N. Intermolecular Hydrogen-Bonded Organic Semiconductors—Quinacridone versus Pentacene. *Appl. Phys. Lett.* **2012**, *101*, 023305.

(10) Chen, L.; Hernandez, Y.; Feng, X.; Müllen, K. From Nanographene and Graphene Nanoribbons to Graphene Sheets: Chemical Synthesis. *Angew. Chem., Int. Ed.* **2012**, *51*, 7640−7654.

(11) Gu, Y.; Muñoz-Mármol, R.; Wu, S.; Han, Y.; Ni, Y.; Díaz-García, M. A.; Casado, J.; Wu, J. Cove-Edged Nanographenes with Localized Double Bonds. *Angew. Chem.* **2020**, *132*, 8190−8194.

(12) Bonal, V.; Muñoz-Mármol, R.; Gordillo Gámez, F.; Morales-Vidal, M.; Villalvilla, J. M.; Boj, P. G.; Quintana, J. A.; Gu, Y.; Wu, J.; Casado, J.; Díaz-García, M. A. Solution-Processed Nanographene Distributed Feedback Lasers. *Nat. Commun.* **2019**, *10*, 3327.

(13) Han, Y.; Xue, Z.; Li, G.; Gu, Y.; Ni, Y.; Dong, S.; Chi, C. Formation of Azulene-Embedded Nanographene: Naphthalene to Azulene Rearrangement During the Scholl Reaction. *Angew. Chem., Int. Ed.* **2020**, *59*, 9026−9031.

(14) Povie, G.; Segawa, Y.; Nishihara, T.; Miyauchi, Y.; Itami, K. Synthesis of a Carbon Nanobelt. *Science* **2017**, *356*, 172−175.

(15) Povie, G.; Segawa, Y.; Nishihara, T.; Miyauchi, Y.; Itami, K. Synthesis and Size-Dependent Properties of [12], [16], and [24] Carbon Nanobelts. *J. Am. Chem. Soc.* **2018**, *140*, 10054−10059.

(16) Nielsen, C. B.; Holliday, S.; Chen, H.-Y.; Cryer, S. J.; McCulloch, I. Non-Fullerene Electron Acceptors for Use in Organic Solar Cells. *Acc. Chem. Res.* **2015**, *48*, 2803−2812.

(17) Yan, C.; Barlow, S.; Wang, Z.; Yan, H.; Jen, A. K.-Y.; Marder, S. R.; Zhan, X. Non-Fullerene Acceptors for Organic Solar Cells. *Nat. Rev. Mater.* **2018**, *3*, 18003.

(18) Shan, B.; Miao, Q. Molecular Design of N-Type Organic Semiconductors for High-Performance Thin Film Transistors. *Tetrahedron Lett.* **2017**, *58*, 1903−1911.

(19) Quinn, J. T. E.; Zhu, J.; Li, X.; Wang, J.; Li, Y. Recent Progress in the Development of N-Type Organic Semiconductors for Organic Field Effect Transistors. *J. Mater. Chem. C* **2017**, *5*, 8654−8681.

(20) Lakshminarayana, A. N.; Ong, A.; Chi, C. Modification of Acenes for N-Channel OFET Materials. *J. Mater. Chem. C* **2018**, *6*, 3551−3563.

(21) Dou, J.-H.; Yu, Z.-A.; Zhang, J.; Zheng, Y.-Q.; Yao, Z.-F.; Tu, Z.; Wang, X.; Huang, S.; Liu, C.; Sun, J.; Yi, Y.; Cao, X.; Gao, Y.; Wang, J.-Y.; Pei, J. Organic Semiconducting Alloys with Tunable Energy Levels. *J. Am. Chem. Soc.* **2019**, *141*, 6561−6568.

(22) Chen, J.; Yang, K.; Zhou, X.; Guo, X. Ladder-Type Heteroarene-Based Organic Semiconductors. *Chem. - Asian J.* **2018**, *13*, 2587−2600.

(23) Wang, Y.; Guo, H.; Ling, S.; Arrechea-Marcos, I.; Wang, Y.; López Navarrete, J. T.; Ortiz, R. P.; Guo, X. Ladder-Type Heteroarenes: Up to 15 Rings with Five Imide Groups. *Angew. Chem.* **2017**, *129*, 10056−10061.

(24) Bunz, U. H. F.; Engelhart, J. U.; Lindner, B. D.; Schaffroth, M. Large N-Heteroacenes: New Tricks for Very Old Dogs? *Angew. Chem., Int. Ed.* **2013**, *52*, 3810−3821.

(25) Lopez, S. A.; Sanchez-Lengeling, B.; de Goes Soares, J.; Aspuru-Guzik, A. Design Principles and Top Non-Fullerene Acceptor Candidates for Organic Photovoltaics. *Joule* **2017**, *1*, 857−870.
(26) Liu, K.; Lalancette, R. A.; Jäkle, F. Tuning the Structure and Electronic Properties of B-N Fused Dipyridylanthracene and Implications on the Self-Sensitized Reactivity with Singlet Oxygen. *J. Am. Chem. Soc.* **2019**, *141*, 7453−7462.
(27) Zhu, C.; Ji, X.; You, D.; Chen, T. L.; Mu, A. U.; Barker, K. P.; Klivansky, L. M.; Liu, Y.; Fang, L. Extraordinary Redox Activities in Ladder-Type Conjugated Molecules Enabled by B ← N Coordination-Promoted Delocalization and Hyperconjugation. *J. Am. Chem. Soc.* **2018**, *140*, 18173−18182.
(28) Vanga, M.; Lalancette, R. A.; Jäkle, F. Controlling the Optoelectronic Properties of Pyrene by Regioselective Lewis Base-Directed Electrophilic Aromatic Borylation. *Chem. - Eur. J.* **2019**, *25*, 10133−10140.
(29) Crossley, D. L.; Cade, I. A.; Clark, E. R.; Escande, A.; Humphries, M. J.; King, S. M.; Vitorica-Yrezabal, I.; Ingleson, M. J.; Turner, M. L. Enhancing Electron Affinity and Tuning Band Gap in Donor-Acceptor Organic Semiconductors by Benzothiadiazole Directed C-H Borylation. *Chem. Sci.* **2015**, *6*, 5144−5151.
(30) Mellerup, S. K.; Wang, S. Boron-Based Stimuli Responsive Materials. *Chem. Soc. Rev.* **2019**, *48*, 3537−3549.
(31) Huang, Z.; Wang, S.; Dewhurst, R. D.; Ignat'ev, N. V.; Finze, M.; Braunschweig, H. Boron: Its Role in Energy-Related Processes and Applications. *Angew. Chem., Int. Ed.* **2020**, *59*, 8800−8816.
(32) Zhuang, F.-D.; Sun, Z.-H.; Yao, Z.-F.; Chen, Q.-R.; Huang, Z.; Yang, J.-H.; Wang, J.-Y.; Pei, J. BN-Embedded Tetrabenzopentacene: A Pentacene Derivative with Improved Stability. *Angew. Chem., Int. Ed.* **2019**, *58*, 10708−10712.
(33) Wang, X.-Y.; Zhuang, F.-D.; Wang, R.-B.; Wang, X.-C.; Cao, X.-Y.; Wang, J.-Y.; Pei, J. A Straightforward Strategy toward Large BN-Embedded π-Systems: Synthesis, Structure, and Optoelectronic Properties of Extended BN Heterosuperbenzenes. *J. Am. Chem. Soc.* **2014**, *136*, 3764−3767.
(34) Min, Y.; Dou, C.; Liu, D.; Dong, H.; Liu, J. Quadruply B←N-Fused Dibenzo-Azaacene with High Electron Affinity and High Electron Mobility. *J. Am. Chem. Soc.* **2019**, *141*, 17015−17021.
(35) Fischer, G. M.; Daltrozzo, E.; Zumbusch, A. Selective NIR Chromophores: Bis(Pyrrolopyrrole) Cyanines. *Angew. Chem., Int. Ed.* **2011**, *50*, 1406−1409.
(36) Shimogawa, H.; Murata, Y.; Wakamiya, A. NIR-Absorbing Dye Based on BF2-Bridged Azafulvene Dimer as a Strong Electron-Accepting Unit. *Org. Lett.* **2018**, *20*, 5135−5138.
(37) Zhu, C.; Guo, Z.-H.; Mu, A. U.; Liu, Y.; Wheeler, S. E.; Fang, L. Low Band Gap Coplanar Conjugated Molecules Featuring Dynamic Intramolecular Lewis Acid-Base Coordination. *J. Org. Chem.* **2016**, *81*, 4347−4352.
(38) Han, Y.; Barnes, G.; Lin, Y.-H.; Martin, J.; Al-Hashimi, M.; AlQaradawi, S. Y.; Anthopoulos, T. D.; Heeney, M. Doping of Large Ionization Potential Indenopyrazine Polymers via Lewis Acid Complexation with Tris(pentafluorophenyl)borane: A Simple Method for Improving the Performance of Organic Thin-Film Transistors. *Chem. Mater.* **2016**, *28*, 8016−8024.
(39) Grandl, M.; Rudolf, B.; Sun, Y.; Bechtel, D. F.; Pierik, A. J.; Pammer, F. Intramolecular N→B Coordination as a Stabilizing Scaffold for π-Conjugated Radical Anions with Tunable Redox Potentials. *Organometallics* **2017**, *36*, 2527−2535.
(40) Grandl, M.; Kaese, T.; Krautsieder, A.; Sun, Y.; Pammer, F. Hydroboration as an Efficient Tool for the Preparation of Electronically and Structurally Diverse N→B-Heterocycles. *Chem. - Eur. J.* **2016**, *22*, 14373−14382.
(41) Wakamiya, A.; Taniguchi, T.; Yamaguchi, S. Intramolecular B-N Coordination as a Scaffold for Electron-Transporting Materials: Synthesis and Properties of Boryl-Substituted Thienylthiazoles. *Angew. Chem., Int. Ed.* **2006**, *45*, 3170−3173.
(42) Min, Y.; Dou, C.; Tian, H.; Geng, Y.; Liu, J.; Wang, L. N-Type Azaacenes Containing B←N Units. *Angew. Chem., Int. Ed.* **2018**, *57*, 2000−2004.
(43) Sun, H.; Guo, X.; Facchetti, A. High-Performance n-Type Polymer Semiconductors: Applications, Recent Development, and Challenges. *Chem.* **2020**, *6*, 1310−1326.
(44) Long, X.; Ding, Z.; Dou, C.; Zhang, J.; Liu, J.; Wang, L. Polymer Acceptor Based on Double B←N Bridged Bipyridine (BNBP) Unit for High-Efficiency All-Polymer Solar Cells. *Adv. Mater.* **2016**, *28*, 6504−6508.
(45) Dou, C.; Long, X.; Ding, Z.; Xie, Z.; Liu, J.; Wang, L. An Electron-Deficient Building Block Based on the B←N Unit: An Electron Acceptor for All-Polymer Solar Cells. *Angew. Chem., Int. Ed.* **2016**, *55*, 1436−1440.
(46) Mula, S.; Leclerc, N.; Lévêque, P.; Retailleau, P.; Ulrich, G. Synthesis of Indolo[3,2-b]Carbazole-Based Boron Complexes with Tunable Photophysical and Electrochemical Properties. *J. Org. Chem.* **2018**, *83*, 14406−14418.
(47) Dou, C.; Ding, Z.; Zhang, Z.; Xie, Z.; Liu, J.; Wang, L. Developing Conjugated Polymers with High Electron Affinity by Replacing a C−C Unit with a B←N Unit. *Angew. Chem., Int. Ed.* **2015**, *54*, 3648−3652.
(48) Koppel, I.; Koppel, J.; Maria, P.-C.; Gal, J.-F.; Notario, R.; Vlasov, V. M.; Taft, R. W. Comparison of Brönsted Acidities of Neutral NH-Acids in Gas Phase, Dimethyl Sulfoxide and Water. *Int. J. Mass Spectrom. Ion Processes* **1998**, *175*, 61−69.
(49) Barłóg, M.; Zhang, X.; Kulai, I.; Yang, D. S.; Sredojevic, D. N.; Sil, A.; Ji, X.; Salih, K. S. M.; Bazzi, H. S.; Bronstein, H.; Fang, L.; Kim, J.; Marks, T. J.; Guo, X.; Al-Hashimi, M. Indacenodithiazole-Ladder-Type Bridged Di(Thiophene)-Difluoro-Benzothiadiazole-Conjugated Copolymers as Ambipolar Organic Field-Effect Transistors. *Chem. Mater.* **2019**, *31*, 9488−9496.
(50) Qiu, F.; Zhang, F.; Tang, R.; Fu, Y.; Wang, X.; Han, S.; Zhuang, X.; Feng, X. Triple Boron-Cored Chromophores Bearing Discotic 5,11,17-Triazatrinaphthylene-Based Ligands. *Org. Lett.* **2016**, *18*, 1398−1401.
(51) Menges, N. Computational Study on Aromaticity and Resonance Structures of Substituted BODIPY Derivatives. *Comput. Theor. Chem.* **2015**, *1068*, 117−122.
(52) Meng, F.; Bu, Y.; Liu, C. Theoretical Study of the Pyridine-BF3 Complex. *J. Mol. Struct.: THEOCHEM* **2002**, *588*, 1−8.
(53) Tao, J.; Sun, D.; Sun, L.; Li, Z.; Fu, B.; Liu, J.; Zhang, L.; Wang, S.; Fang, Y.; Xu, H. Tuning the Photo-Physical Properties of BODIPY Dyes: Effects of 1, 3, 5, 7- Substitution on Their Optical and Electrochemical Behaviours. *Dyes Pigm.* **2019**, *168*, 166−174.
(54) Yang, J.; Cai, F.; Desbois, N.; Huang, L.; Gros, C. P.; Bolze, F.; Fang, Y.; Wang, S.; Xu, H.-J. Synthesis, Spectroscopic Characterization, One and Two-Photon Absorption Properties and Electrochemistry of π-Expanded BODIPYs Dyes. *Dyes Pigm.* **2020**, *175*, 108173.
(55) Ie, Y.; Ueta, M.; Nitani, M.; Tohnai, N.; Miyata, M.; Tada, H.; Aso, Y. Air-Stable n-Type Organic Field-Effect Transistors Based on 4,9-Dihydro-s-Indaceno[1,2-b:5,6-B′]Dithiazole-4,9-Dione Unit. *Chem. Mater.* **2012**, *24*, 3285−3293.

https://dx.doi.org/10.1021/acs.joc.0c02052
J. Org. Chem. 2021, 86, 2100−2106